Precise characterization of the Performance of CHARM-F during Ground-based and Airborne Measurements

Mathieu Quatrevalet¹, Christian Fruck¹, Martin Wirth¹,
Christian Büdenbender¹, Christoph Kiemle¹,
Nina Burgdorfer¹, Sebastian Wolff ¹, Gerhard Ehret¹,
Andreas Fix¹

Deutsches Zentrum für Luft- und Raumfahrt (DLR), Institut für Physik der Atmosphäre, 82234 Oberpfaffenhofen, Germany, E-mail: mathieu.quatrevalet@dlr.de

Abstract. CHARM-F (CO₂ and CH₄ atmospheric remote monitoring - Flugzeug) is a lidar system for airborne measurements of carbon dioxide and methane, using the integrated path differential absorption (IPDA) technique. It serves as a demonstrator, testbed and validation tool for the upcoming MERLIN mission and for future airborne or spaceborne lidars for anthropogenic greenhouse gases. It has been deployed on three flight campaigns since 2015, and is still being improved and further characterized under lab conditions and on a test range in order to better understand and reduce instrumental biases. We report here on the current status of our understanding of the instrument performance, and show some recent results. We also introduce our plans for the CoMet 2.0 campaign that will take place this summer (2022) over northern Canada and Alaska. Keywords: Airborne, Dial, IPDA, CO₂, CH₄, MERLIN.

1 Context

DIfferential Absorption Lidar (DIAL) is a promising technology for remote sensing of the three main climate-relevant, long-lived anthropogenic greenhouse gases: carbon dioxide, methane and nitrous oxide [1]. In 2008, building on the success of its airborne DIAL system for water vapour, the Institute for Atmospheric Physics of the German Aerospace Centre started the design and subsequent assembly of CHARM-F, an IPDA lidar instrument for simultaneous measurements of the column-averaged mixing ratios of carbon dioxide and methane, XCO2 and XCH4. Approximately at the same time, the Methane Remote sensing LIdar mission (MERLIN), a French-German initiative to build a spaceborne IPDA lidar for methane was initiated [2]. CHARM-F naturally endorsed the role of technology demonstrator, testbench and future validation tool for MERLIN. While awaiting the launch of MERLIN, CHARM-F has been and will be enrolled in a number of flight campaigns to further the technological maturity and to provide IPDA data for inverse modelling experiments to the climate science community, so far used to working with data from passive instruments.

2 Instrument, platforms and campaigns

CHARM-F's architecture and specifications have been described in more details in a previous ILRC contribution [3]. The system consists of two largely independent lidar systems operating near 1.57 um for carbon dioxide and near 1.64 nm for methane. The transmitters are built around injection-seeded Optical Parametric Oscillators (OPO) that are pumped by diode-pumped, injection seeded, and Q-switched Nd:YAG lasers in a master-oscillator power-amplifier configuration. They produce double pulses separated by 500 µs at a pulse pair frequency of 50 Hz, whereby one pulse is emitted at the so-called online wavelength on an absorption line of the trace gas, and the other at the offline wavelength. This is achieved by seeding the OPOs alternatively with two seed lasers using a fast, solid-state optical switch. The seed lasers, telecom-type, Distributed Feedback (DFB) semiconductor lasers or fiber lasers, are offset-locked to reference DFB lasers that are themselves stabilized using a gas absorption cell. against the same absorption lines that are used in the atmosphere for the IPDA measurement.

There are two independent receivers per trace gas, which proved decisive to detect and quantify instrumental biases, as will become clear in paragraph 3.3. One receiver consists of an InGaAs, four-quadrant, 1-mm PIN photodiode in the focal plane of a 20-cm aperture telescope, the other is based on a 0.2-mm InGaAs Avalanche Photodiode (APD), in the focal plane of an aperture imaging, 6-cm objective. Both provide a field of view of 3.3 mrad. A relative pulse energy calibration path redirects a very small fraction of the outgoing pulses to the receiver's detectors.

CHARM-F was originally designed to fly onboard DLR's flagship research aircraft, HALO (High-Altitude, LOng-range), a modified Gulfstream V. It has accumulated about 85 flight hours within Europe so far on this platform, first in the frame of an instrumental test campaign in 2015 and then in the frame of the Comet 1.0 campaign in 2018. In 2021, CHARM-F was also adapted to be flown on the ATR-42 of the French facility for airborne research (Safire), in order to be able to take part in the MAGIC2021 campaign in Northern Sweden. Some very preliminary results from the latter campaign can be found in the contribution of Cézard et al to this year's conference.

3 Recent results and discussion of instrument performance

3.1 Quantification of emission rates from a regional cluster of point sources

We previously reported on the ability of CHARM-F to detect and quantify carbon dioxide plumes from large coal-fired power plants, which were among the targets of the CoMet 1.0 campaign [5]. Another major focus of the campaign was the Upper Silesian Coal Basin (USCB) in Southern Poland, one of the main sources of anthropogenic methane emissions in Europe via the ventilation shafts of its coal mines.

Fig. 1 shows preliminary results from an on-going study aiming at retrieving the emission rates from the individual ventilation shafts, and eventually the total regional emissions, using the CHARM-F observations acquired on our "golden day" for the USCB on June 7th, 2018, a flight consisting of many transects of the USCB across the main wind direction. The study makes use of a ventilation shaft inventory with prior emission rates compiled for CoMet; a transport model, the Weather Research Forecast (WRF); and a framework, the CarbonTracker Data Assimilation Shell (CTDAS), to determine optimized emission rates that minimize a cost function composed of the mean error with respect to the observations and of the mean error with respect to the prior emissions of the shafts.

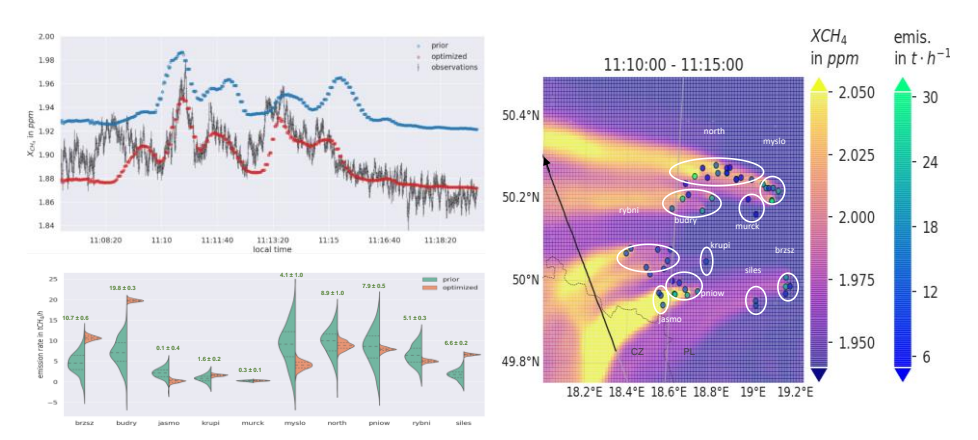


Fig. 1. Right: map of ventilation shafts and their emission rates in the USCB (right), and a snapshot of the modelled regional methane plumes at the time of the overflight. Upper left: example transect (black arrow on the map) with prior and optimized XCH4, and CHARM-F observations. Lower left: prior and optimized total emissions from the subsets of shafts defined on the map with white circles, with corresponding prior and optimized uncertainties.

The example transect shown here demonstrates that CHARM-F convincingly captures all expected methane plumes, plus a source that is missing from the inventory at the beginning of the transect. Also interesting is a plume in the middle of the transect which is crossed earlier than in the model, likely due to an incorrect wind field. Overall, it can be seen that the CHARM-F data contains information that has a large impact on the optimized emission rates, resulting itself in a large uncertainty reduction.

3.2 Inter-receiver, time-varying biases

While the performance of CHARM-F already enables promising scientific exploitation of the data as shown in previous publications and in the previous paragraph, closer cross-examination of the XCO2 and XCH4 time series within each pair of receivers reveals remaining issues with instrumental artefacts, as shown on Fig. 2 for methane.

To various degrees depending on the flight, the measurements are affected by interreceiver biases, ranging from almost none on our "golden day" for the USCB (lowermost case on Fig. 2) up to 2-3 percent in the worst case (uppermost case). These biases show variations over timescales of a few minutes to a few hours, and also depend on the seeding order within a pulse pair, on/off or off/on, which is flipped from one pair to the next precisely in order to reduce biases due to possible asymmetries in the properties of the first and second pulse, as already explained in [4].

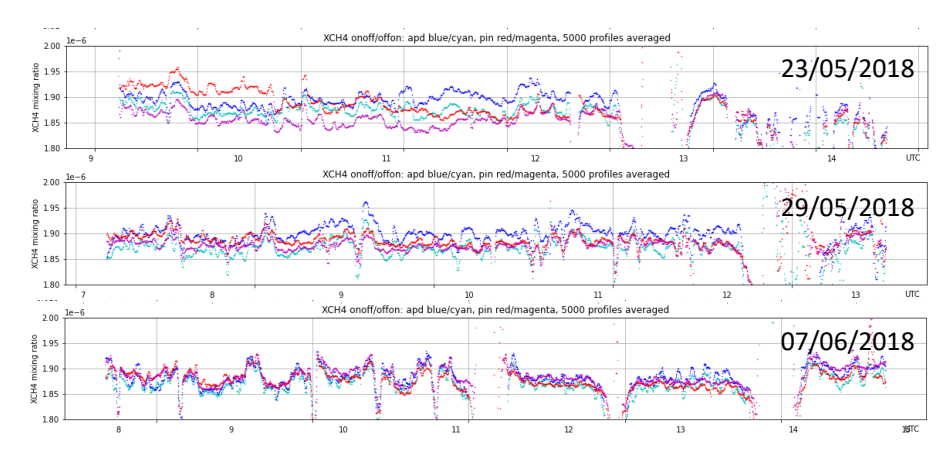


Fig. 2. Time series of XCH4, with a gliding average of 100s, for three exemplary flights of Comet 1.0, retrieved using the PIN signals and the on/off, respectively off/on pulse pairs (red resp. magenta), or using the APD signals and the on/off, respectively off/on pairs (blue resp. cyan).

Our current working theory is that these inter-receiver biases are mainly caused by the combination of a field-dependent response of the receivers, and of time-varying differences in the far-field beam cross-sections of the four "pulse types": on1, on2, off1 and off2. Field dependency in the receivers may arise in particular from the angle-dependency of the 2-nm bandpass filters, of from spatial non-uniformities of the detector responsivity. This is especially true for the four-quadrant PIN photodiode, owing to the 30-micron gaps between the four quadrants. Differential clipping of even a small portion of the laser footprint by the receiver's field of view may also produce the same effect, in which case it correlates with laser pointing variations.

4 On-going ground-based activities

4.1 Characterization of inter-pulse laser beam cross-section differences

In light of the considerations summarized in paragraph 3.2, special attention is now given to the beam profile differences between the four pulse types during the necessary realignment of the lasers between campaigns. Long-term observation of the running lasers in the laboratory show that inter-pulse beam profile differences, unfortunately,

change over time in a continuous way from the point in time where the laser is switched on. Fig. 3 shows an example of this time-dependency for the methane transmitter.

While it is possible to align the laser so that the working point after sufficient warm-up time minimizes the differences, the laser is sensitive to its thermal environment and thermal cycling may shift it to another working point, which, together with pointing variations, may also explain the observed evolutions of the biases (Fig. 2).

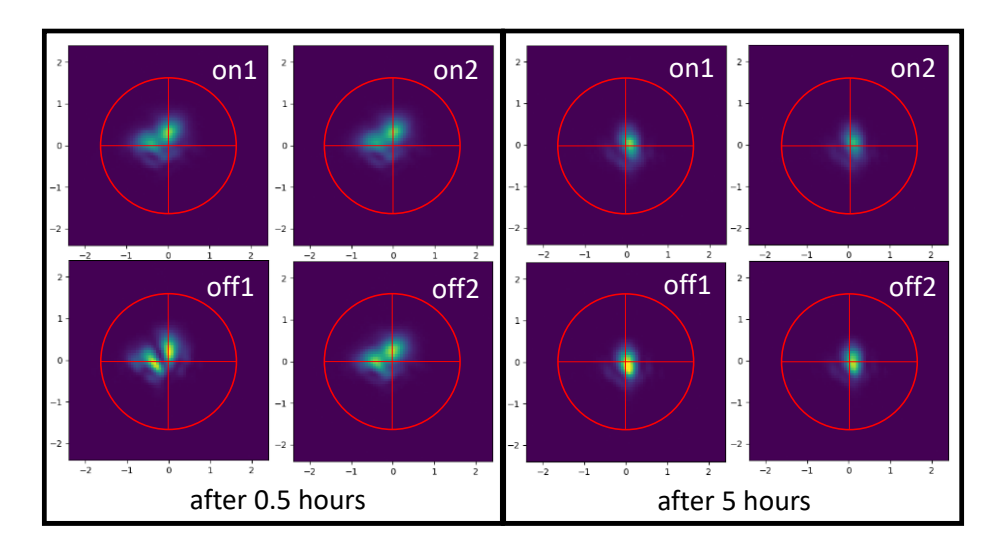


Fig. 3. Far-field laser beam cross-sections of the CHARM-F transmitter at 1.64 micron, after different running times from switch-on. The x and y scales are in milliradians, red circles simulate the receivers' field of view, red lines the gaps between the four quadrants of the PIN diode.

4.2 Test range implementation

In order to quantify the impact of the afore-mentioned laser behavior and look into ways to minimize it, controlled measurements that mimic the in-flight viewing geometry are necessary, with a distance to the scattering surface large enough so that the laser beam can be considered to have reached the far-field mode. The Institute for Atmospheric Physics in Oberpfaffenhofen happens to lie at the western edge of an airfield, with one laboratory room of the institute conveniently located at the eastern end of the building, providing a free line-of-sight over the airfield to a large forested area on its eastern, 2 to 3 kms away.

In the past, experiments have been made using the trees themselves as targets [6]. However, the heterogenous ground reflectivity distribution seen by the instrument in flight displays no long-term correlation at timescales longer than a few pulse pairs, so that this effect only adds white noise that can be reduced with averaging, as explained in [7]. Trees as seen from a fixed position, on the contrary, are heterogenous targets that move slowly around an average position, giving rise to the same effect as variations of the laser intensity distribution at the target. This conceals the intrinsic instrumental

effects, and averaging is not effective. Therefore, there is a need for either a nonuniform but rapidly moving, or a fixed but uniform target.

Since the 3,3 mrad field of view translates to a diameter of 5,5 meters at 1,6 km, the distance to the location within the airfield where we are allowed to set up a target as shown on the map of Fig. 4, practical considerations call for a fixed, uniform target, which we were able to procure in the form of an inflatable screen with a reflective white PVC surface of 7x7m, also visible on Fig. 4. It is expected that this test range will help to further our understanding of the inter-receiver biases. and better align the system for future campaigns.



Fig. 4. From left to right: view from the laboratory window, location of the test range in Ober-pfaffenhofen and 7x7m inflatable reflective screen ready for use.

5 Upcoming flight campaign: CoMet 2.0 Arctic

So far, the emphasis of CHARM-F's deployments has been put on anthropogenic emissions of CO₂ and CH₄. In an upcoming field campaign in summer of 2022, CHARM-F will be part of a comprehensive payload consisting of remote sensing and in-situ instruments onboard HALO. The goal of this campaign, CoMet 2.0 Arctic, is to estimate methane fluxes of large wetlands in the North American arctic and boreal regions and separate natural and anthropogenic fluxes (e.g. from oil and gas excavation) of this important greenhouse gas.

References

- Ehret, et al, 2008: Space-borne remote sensing of CO2, CH4, and N2O by integrated path differential absorption lidar: a sensitivity analysis, Appl. Phys. B volume 90, pages 593–608
- 2. Ehret et al, 2017: MERLIN: A French-German Space Lidar Mission Dedicated to Atmospheric Methane, Remote Sens., *9*, 1052.
- Quatrevalet et al, 2010: CHARM-F: The Airborne Integral Path Differential Absorption Lidar for Simultaneous Measurements of Atmospheric CO2 and CH4, 25th International Laser Radar Conference.

- 4. Amediek et al, 2017: CHARM-F, a new airborne integrated-path differential-absorption lidar for carbon dioxide and methane observations: measurement performance and quantification of strong point source emissions, Appl. Opt., 56(18), 5182-5197.
- 5. Wolff et al, 2021: Determination of the emission rates of CO2 point sources with airborne lidar, Atmospheric Measurement Techniques (AMT), 14 (4), pp. 2717-2736.
- 6. Amediek et al, 2008: Development of an OPO system at 1.57 μm for integrated path DIAL measurement of atmospheric carbon dioxide. Appl. Phys. B (92), pp. 295-302.
- 7. Amediek et al, 2009: Airborne lidar reflectance measurements at 1.57 µm in support of the A-SCOPE mission for atmospheric CO2, Atmos. Meas. Techniques 2(2), 755-772